Optical Transpose Interconnection System Architectures

W. Pijitrojana
Department of Electrical Engineering, Faculty of Engineering,
Thammasat University, Klongluang, Pathumthani 12121, Thailand
Phone 0-2564-3001-9 Ext. 3045, Fax 0-2564-3010,
E-mail: pwanchai@engr.tu.ac.th

T. J. Hall
School of Information Technology & Engineering,
University of Ottawa, 800 King Edward, Ottawa, Ontario K1N 6N5, Canada
Email: thall@site.uottawa.ca

Abstract

An interconnection pattern corresponding to a transposition arises naturally when a connection is required between a set of modules in a stage and a second set of modules. The optical transpose interconnection system (OTIS) was first proposed by Gary C. Marchand *et al.* and has been exploited in a FAST-Net demonstrator by P. Milojkovic *et al.* These implementations employed a scheme based on off-axis imaging. This paper aims to propose an alternative non-imaging scheme of the optical transpose interconnection system by interposing a macrolens, a Fourier transform lens, between the two stages of mesolens arrays. This scheme is shown to be superior in several respects. In order to describe a transposition of the coordinates of input beamlets to the coordinates of output beamlets, the ray of light through the optical system will be represented by points specified by p, the direction cosine, and q, the position, in phase space. The system is useful for implementation of three-stage Clos Networks, the Optical Transpose Sector Switch (OTSS), a reconfigurable Optical Transpose system, and an Optical Crossbar Switch.

Keywords: Free space optical interconnection, Fourier transform lens, matrix optics, phase space, network switch.

1. Introduction

Electrical interconnection becomes a bottleneck for the communication of information at long distances and high bit rates. Free space optical interconnection offers several potential advantages for implementing communication with large data bandwidths, high bandwidth, low skew and cross talk, small volume, high connection density, and lower power consumption [1,2]. Thus optical interconnects may overcome the present limitations of electrical interconnects in a simple and cost-effective manner.

Interconnection may be thought of as a mapping, one-to-one or possibly one-to-many, from the set of sources to the set of receptors. In this paper we proposed an improved one-to-one Optical Transpose Interconnection System. An optical transpose interconnection system (OTIS), which is described in Ref. 3, has two stages each consisting of an array of lenslets that image the light from an array of light sources on an input plane onto an array of receivers on an output plane. The system suffers from severe aberration due to the off-axis imaging arrangement of similar sized lenslets. As described, the light strikes the second lenslet plane off-center, partially filling an adjacent lenslet, focusing to a different receiver. This effect leads to high insertion loss and potential for cross talk if the light not captured is not fully blocked. Spatially coherent sources individually directed into the appropriate lenslet could overcome these problems but would require beam steering components at the input plane and also, in the monomode receiving device, at the output plane. The other OTIS is the FAST-Net optical system described in Ref. 4. The unfolded

system uses arrays of wide field-of-view imaging lenses. In order to map an image of each source on input plane onto a corresponding receiver on output plane, the source spacing on the array has to be matched to the lens array. This effect makes the whole system not have simply one optical axis. The system also suffers from aberration because the angles between the VCSELs, on one corner of the array, beam and the optical axis of the lens exceeded 20°, wide angle. The system proposed in this paper is an improved system in which interposing a macrolens, a Fourier transform lens, between the two stages of microlens arrays with elements in different arrangement. The system does not require beam steering components and it is simple to arrange the input and output devices.

2. Fundamental Theory of the OTIS system

The transpose interconnection is a one-to-one interconnection between $N \times M$ input beamlets to $N \times M$ output beamlets. The input and output beamlets are arranged as an $\sqrt{N} \times \sqrt{M}$ array with $\sqrt{N} \times \sqrt{M}$ sub-array. Each $\sqrt{N} \times \sqrt{M}$ sub-array of input and output beamlets are at the front and back focal planes of each of lenses of stage I and III which are arranged as an $\sqrt{N} \times \sqrt{M}$ array. Each input and output beamlets has a coordinate (n,m) where $n,m = 1,...,\sqrt{N} \times \sqrt{M}$. The input beamlet with the coordinate (n,m) is mapped to the output beamlet with the coordinate (m,n), called the transposition of the input. We can write this as the equation:

$$(n,m) \rightarrow (m,n) \qquad (1)$$

In our analysis the sources of input beamlets are considered to be telecentric sources, i.e. the chief ray of each source is parallel to the optical axis of the corresponding lens in stage I. The microlenses in stage I are positioned one focal length away from the sources. The macrolens in stage II and microlenses array in stage III are positioned as shown in Figure 1(b) so that the images of the input beamlets can be Fourier transformed at the output. Figure 1 shows the diagram of the system for N and M = 16. The system composites of 256 input and output beamlets arranged as a 4×4 array with 4×4 sub-array, a 4×4 array of lenses in stage I, a macrolens in stage II, and an 4×4 array of lenses in stage III. The input beamlet with coordinate (1,1), for example, on the microlens n = 1 in stage I is mapped to the output beamlet with coordinate (1,1) on the microlens n = 1 in stage III, similarly the input beamlet with coordinate (1,2) on the microlens n = 1 in stage I is mapped to the output beamlet with coordinate (2,1) on the microlens n = 2 in stage III, and so on.

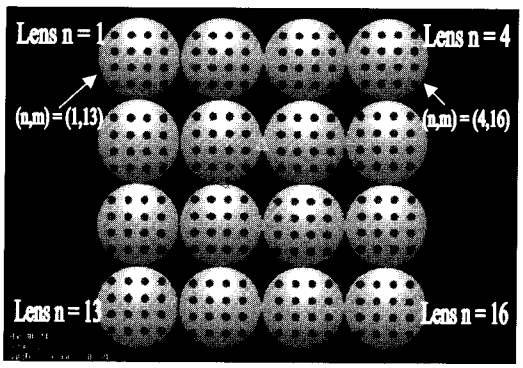

Coordinates of lenses and inputs in stage I

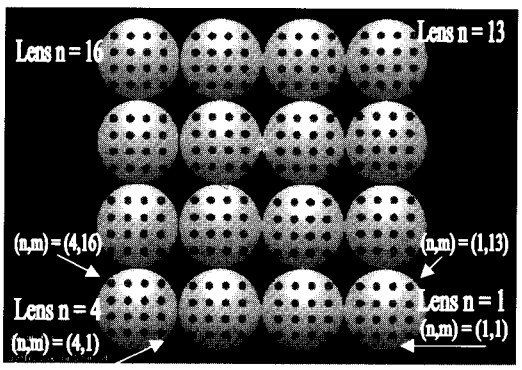

Coordinates of lenses and outputs in stage III
(a) Front View of inputs, outputs, and mesolenses in stage I and III.

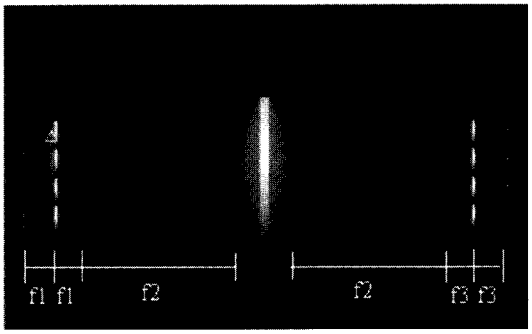

Side View of layout of the OTIS system

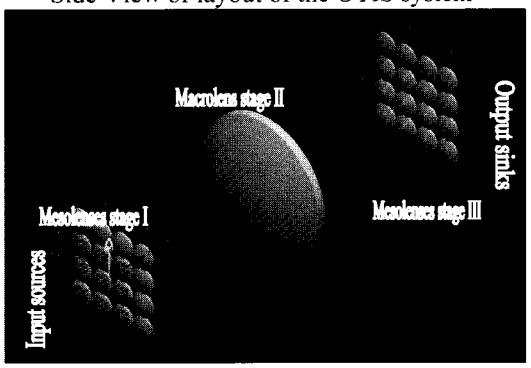

Isometric View of layout of the OTIS system
(b) Layout of the OTIS system

Figure 1. Diagram of the OTIS system with $N = M = 16$.

The nature of the optical transpose interconnection system can be described theoretically as follows: The ray of light from the input source can be represented by points. The points where the ray intersects the plane transverse to the z-axis can be specified by the position, (q_x, q_y), and the direction of the ray, (γ_x, γ_y). We can replace the direction of the ray by p variable, where $p_x = n\sin\theta_x$ and $p_y = n\sin\theta_y$. In optical phase space the ray of light propagates from the point u_1 at the reference plane at z_1 to the point u_2 at the reference plane at z_2, the ray will correspond to vectors:

$$u_1 = \begin{pmatrix} q_{x1} \\ q_{y1} \\ p_{x1} \\ p_{y1} \end{pmatrix} = \begin{pmatrix} q_1 \\ p_1 \end{pmatrix} \text{and } u_2 = \begin{pmatrix} q_{x2} \\ q_{y2} \\ p_{x2} \\ p_{y2} \end{pmatrix} = \begin{pmatrix} q_2 \\ p_2 \end{pmatrix} \quad (2)$$

The relationship between these two points can be described by finding u_1 as a function of u_2. In Geometrical Optics we know that

$$u_1 = \begin{pmatrix} A & B \\ C & D \end{pmatrix} u_2 = Mu_2 \quad (3)$$

where M are 2×2 matrices of determinant 1. These kinds of matrices are called (linear) canonical transformations or symplectic transformations. Any refracting lens system can be considered as the composite of several systems of two basic types:

(a) A translation by a distance t, the formula is:

$$\begin{pmatrix} q_2 \\ p_2 \end{pmatrix} = \begin{pmatrix} 1 & T \\ 0 & 1 \end{pmatrix} \begin{pmatrix} q_1 \\ p_1 \end{pmatrix}$$

$$\det \begin{pmatrix} 1 & T \\ 0 & 1 \end{pmatrix} = 1, \quad T = t/n \quad (4)$$

where n is the refractive index of the medium.

(b) Refraction at the boundary surface between two regions of refractive indices n_1 and n_2, the formula is:

(c)

$$\begin{pmatrix} q_2 \\ p_2 \end{pmatrix} = \begin{pmatrix} 1 & 0 \\ -\rho & 1 \end{pmatrix} \begin{pmatrix} q_1 \\ p_1 \end{pmatrix}$$

$$\det \begin{pmatrix} 1 & 0 \\ -\rho & 1 \end{pmatrix} = 1, \quad \rho = \frac{n_2 - n_1}{R} \quad (5)$$

where R is the radius of the refracting surface.

From these two results, we can calculate the matrix of the thin lens (a double convex lens) between a reference plane F_1 located a distance f (a focal length of the thin lens) to the left of the lens and a reference plane F_2 located a distance f to the right, then we have:

$$\begin{pmatrix} q_2 \\ p_2 \end{pmatrix} = \begin{pmatrix} 0 & f \\ -1/f & 0 \end{pmatrix} \begin{pmatrix} q_1 \\ p_1 \end{pmatrix} \quad (6)$$

where $\frac{1}{f} = (n_2 - n_1)\left(\frac{1}{R_1} - \frac{1}{R_2}\right)$, R_1 is the radius of the left refracting surface and R_2 is the radius of the right refracting surface. From equation (6), the elements A and D of the matrix are zeros. This means there are two cases we will consider as: 1) D = 0. This means that all rays entering the input plane from the same point emerge at the output plane making the same angle with the axis, no matter at what angle the rays enter the system. In another words, the position of the ray is transformed into an angle. 2) A = 0. This means that all rays entering the system at the same angle will pass through the same point in the output plane. Therefore, the angle is transformed into the position of the ray [5]. With two cases it shows that the lens system transforms the coordinate system (q, p) by rotating the axes by 90°:

$$(q, p) \rightarrow (-p, q) \quad (7)$$

Therefore, the optical transpose interconnection system composite of 3 stages of lenses transforms the input beamlets with coordinates $\begin{pmatrix} q \\ p \end{pmatrix}_{nm}$ into the coordinates of the output beamlets $\begin{pmatrix} q \\ p \end{pmatrix}_{mn}$ Equation (8) below is the equation of the system:

$$\begin{pmatrix} q \\ p \end{pmatrix}_{nm} = \begin{pmatrix} 0 & -\frac{f_1 f_3}{f_2} \\ \frac{f_2}{f_1 f_3} & 0 \end{pmatrix} \begin{pmatrix} q \\ p \end{pmatrix}_{mn} \quad (8)$$

or

$$\begin{pmatrix} q \\ p \end{pmatrix}_{nm} = \begin{pmatrix} -\frac{f_1 f_3}{f_2} p \\ \frac{f_2}{f_1 f_3} q \end{pmatrix}_{mn} \quad (9)$$

where $f_1, f_2,$ and f_3 are the focal lengths of lenses in stage I, II, and III, respectively, and the effective focal length of the system is $\frac{f_1 f_3}{f_2}$. By Gaussian beam analysis and linear optical design the optical transpose interconnection system has been designed and simulated as shown in Figure 2. Figure 2 shows the simulation of the system for $N = M = 16$, i.e. the system composites of 256 inputs and outputs. He-Ne laser or VCSELs are the sources of input beamlets with the beam waist ω_0 and the wavelength λ.

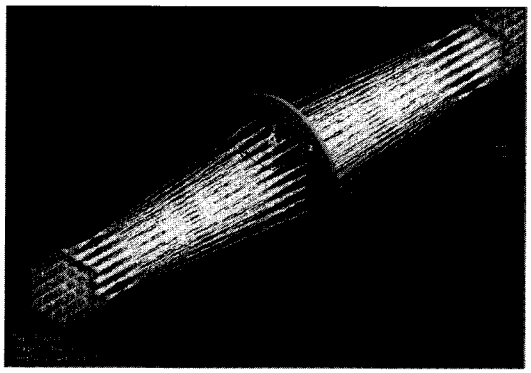

Figure 2. Modelling of the OTIS system.

3. Linear Optical System Design

The key new aspect introduced in this section is that of diffraction albeit in the Gaussian approximation. Three characteristics that characterise Gaussian beam propagation are: (*i*) the phase front curvature and the beam radius in terms of the distance from the beam waist (the minimum beam radius); (*ii*) the propagation of a Gaussian beam in free space; (*iii*) the transformation of a Gaussian beam through a lens. Geometrical representations of these characteristics highlight the relationship between Gaussian beam propagation and geometrical optics. These characteristics of Gaussian beams are applied to the OTIS system to derive the linear optical system design. All lenses used in the OTIS system are off the shelf with $f_{\#1}, f_{\#2}$, and $f_{\#3}$, and d_1, d_2, and d_3 are the f-number and the diameters of lenses in stage I, II, and III, respectively. The pitch of

each input beamlet is δ_1 and the pitch of each output beamlet is δ_3. Let w_1 be the beam waist of the input beamlet at the focal point of microlens in stage I. The effective focal length of the system is:

$$f_{eff} = \frac{\pi w_1^2}{\lambda} \tag{10}$$

The pitch of the sources within an input sector of the microlens in stage I is:

$$\delta_1 = \frac{\pi w_1^2}{\lambda f_{\#1}} \tag{11}$$

The diameters and focal length of lenses in stage I, II, and III are:

$$\begin{aligned} d_1 &= \sqrt{2}\sqrt{M}\delta_1 \\ d_2 &= \sqrt{2}\eta_2(2d_1' + 3d_1) \\ d_3 &= \sqrt{2}\sqrt{N}\delta_3 \end{aligned} \tag{12}$$

where $d_1' = \dfrac{f_2 \sin\theta_f}{\sqrt{1-2\sin^2\theta_f}}$ and

$$\begin{aligned} \theta_f &= \tan^{-1}\left(\frac{(\sqrt{M}-1)\delta_1}{\sqrt{4f_1^2 + [(\sqrt{M}-1)\delta_1]^2}}\right) \\ f_1 &= \eta_1\sqrt{2}\sqrt{M}\frac{\delta_1}{\delta_3}f_{eff} \\ f_2 &= 2\eta_1\eta_3\sqrt{M}\sqrt{N}f_{eff} \\ f_3 &= \eta_3\sqrt{2}\sqrt{N}\frac{\delta_3}{\delta_1}f_{eff} \\ \tan\alpha &= \frac{1}{2}\frac{\sqrt{2}\sqrt{N}d_1}{f_2} \\ \tan\beta &= \frac{1}{2}\frac{\sqrt{2}\sqrt{M}d_3}{f_2} \end{aligned} \tag{13}$$

where η_1, η_2, and η_3 are the microlens, the macrolens, and the microlens margin factors, respectively. α is the field of view of the macrolens from the microlens in stage I and β is the field of view of the macrolens from the microlens in stage III.

4. Simulations and Experiments

The simulations and experimental demonstration of the OTIS system are done with the parameters from the calculation using the equations of the linear optical design. The system is taken to have square dimensions with $N = M = 16$ the input and output beamlets. Therefore, the 256 input and output beamlets are arranged as 4×4 sub-arrays. Each sub-array of input and output beamlets is placed at the front focal point of microlens in stage I and the back focal point of the microlens in stage III, respectively. The number of microlenses in stage I and microlenses in stage III are 16 Fourier transform lenses arranged as 4×4 arrays. The macrolens in stage II is a Fourier transform lens. The f-numbers of the microlenses in stage I and III are selected to be 2.9 (off the shelf lenses) and the beam waist of the light source is 30.57 μm (Specification of He-Ne laser). The wavelength of the light source is 632.8 *nm*. The pitch margin factor of the microlenses in stages I and III, $\eta_1 = \eta_3$, is set to one and the pitch margin of the macrolens in stage II, η_2, is 1.305. The parameters obtained from calculations are as the following:

- $\delta_1 = \delta_3$ the pitch of the input and output beamlets within input and output sectors is 1.6 *mm*.
- f_{eff} the effective focal length of the optical system is 4.62 *mm*.
- $f_1 = f_3$ the focal length of microlens in stage I and microlens in stage III is 26.02 *mm*.
- f_2 the focal length of macrolens is 147.2 *mm*.
- $d_1 = d_3$ the diameter of microlens is 8.97 *mm*.
- $\alpha = \beta$ the field of view is 10°.

The dimensions and optical characteristics of the lenses used in the LightTools [6] simulation correspond to off the shelf lenses used in the experimental demonstration. The lens specifications are as follows:

Stage I Microlens:
Material: BK7_SCHOTT [7]
Element shape: Circular Thickness: 2.74 *mm*
Edge Thickness: 1.99672 *mm* Diameter: 9.0 *mm*
Shape of Front Surface: Spherical
Shape of Rear Surface: Spherical
Radius of Front Surface: 27.43 *mm*
Radius of Rear Surface: 27.43 *mm*

Stage II Macrolens:
Material: BK7_SCHOTT [7]
Element shape: Circular Thickness: 19.5 *mm*
Edge Thickness: 3.10674 *mm* Diameter: 100 *mm*
Shape of Front Surface: Spherical
Shape of Rear Surface: Spherical
Radius of Front Surface: 156.6 *mm*
Radius of Rear Surface: 156.6 *mm*
Stage III Microlens:
Material: BK7_SCHOTT [7]
Element shape: Circular Thickness: 2.74 *mm*
Edge Thickness: 1.99672 *mm* Diameter: 9.0 *mm*
Shape of Front Surface: Spherical
Shape of Rear Surface: Spherical
Radius of Front Surface: 27.43 *mm*
Radius of Rear Surface: 27.43 *mm*
Figure 2 shows the modeling of the OTIS system. Figure 3 shows the experimental setup of the OTIS system. Two of the output images of the microlens in stage III are shown in Figure 4 and 5.

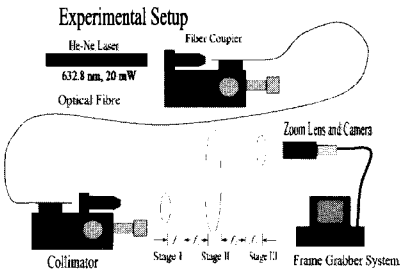

Figure 3. The experimental setup of the OTIS System.

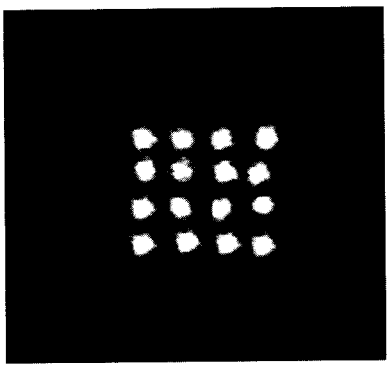

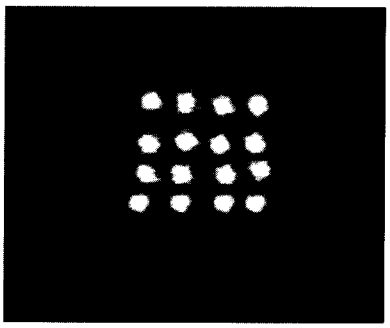

Figure 4 The output images of the 11th microlens in stage III.

Figure 5. The output images of the 16th microlens in stage III.

5. The applications of OTIS system

The optical transpose interconnection system discussed in this paper is fundamental to arbitrary optical interconnection such as a Transpose Sector Switch, a reconfigurable Optical Transpose System, and Optical Crossbar Switch. A Transpose Sector Switch is local fan-out sections, per-input sector transpose sections, bus transpose sections, per-output sector transpose sections, and local fan-in sections as shown in Figure 6.

Reconfiguration techniques are used to allocate hardware resources, such as processors and communication switches, to a specific task. The hardware resources allocated are usually interconnected to form a suitable network topology for the task. Figure 7 shows a Reconfigurable Cross Connect system.

A crossbar switch is a switch which can be used to interconnect any one of a plurality of inputs to any one of a plurality of outputs. Figure 8 shows a topologically equivalent switch of the optical crossbar switch.

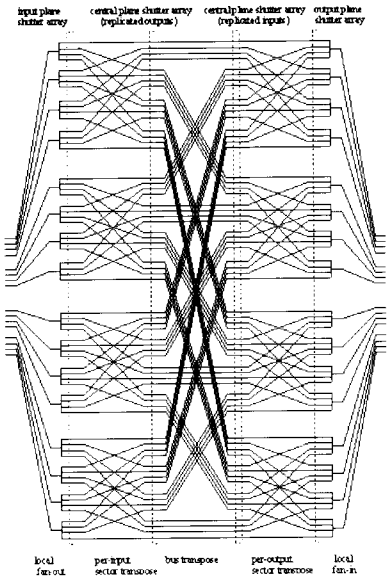

Figure 6. A Transpose Sector Switch.

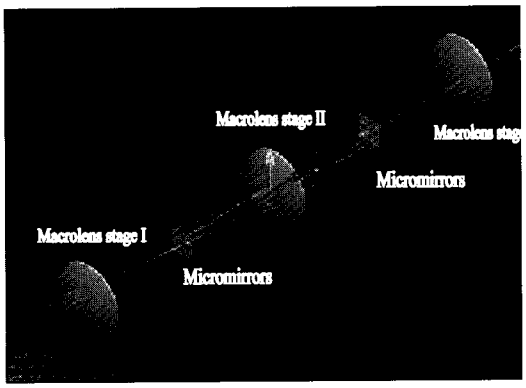

Figure 7. A Reconfigurable Cross Connect system using micromirrors in stage I and III.

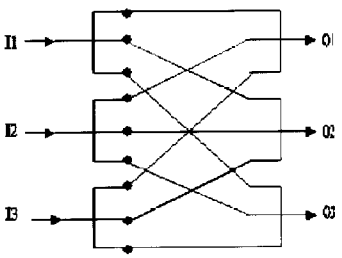

Figure 8. An topologically Optical Crossbar Switch.

6. The Scaling Laws of the Optical System

The motivation of this section is to consider how to pack the channels as densely as possible and also to make the distance between the input and output planes as small as possible. Interconnection systems are considered as imaging optical systems. Therefore, the scaling law for the optical systems is related to the lens system. Lenses come in many different sizes. Those used in common optical instruments and systems have dimensions of the order of centimeters. However, the very small lenses required · by optical computing and interconnection systems can be measured in micrometers. The lens system design, one of the influences of scaling is on the number of data channels, which can be handled in parallel. The space-bandwidth product SW is proportional to the number of data channels. Hence, the SW is an appropriate measure of the system quality and a key criterion for the usefulness of the free-space optical interconnects system. The SW can be interpreted as the number of degrees of freedom of the wave field at the exit of the lens system and also as the number of resolvable points in the image plane. The conclusion is that large diameters and large f-number maximize the space bandwidth product. Large f-numbers increase the diffraction spot with respect to the size of a wavelength but reduce the aberration spot, but large diameters increase the aberration spot and can tend to dominate the diffraction spot. The use of many small lenses rather than a single large lens can maximize the overall information density of the system. Reducing the diameter reduces the aberration spot down to the size of the diffraction spot, resulting in the smallest possible overall spot size. The field size is also small, but this is compensated for by the fact that the small diameter of the lens enables many such systems to be used in parallel. Thus the overall information density is maximized with many small tubes rather than by a single lens.

In optical interconnection architectures, the input and output channels are arranged as arrays in a regular Cartesian manner at the input and output planes. The cross section of the optical channel links between a pair of 2-D input-output planes is approximately equal to $\lambda^2/2\pi$. It has been further shown that the basic 3-D volume for establishing such free-space communications

is $(\lambda^2/2\pi)L_{total}$, where L_{total} is the total length of communication channels [13].

The minimum effective focal length of the OTIS is:

$$f_{eff,\min} = \frac{4\lambda}{\pi} f_{\#1} f_{\#3} \tag{14}$$

The total linear length of the OTIS with the total input point NM is given as:

$$L_{total} = \frac{8\lambda}{\pi}\left(\frac{2m+4}{m}\right)\eta_1\eta_2 NM\sqrt{N}\sqrt{M} f_{\#1} f_{\#3} \tag{15}$$

From [13], the total volume that must be allocated for optical communication must at least be given as $V \geq \frac{\lambda^2}{2\pi} L_{total}$. Therefore, the lower bound of the optical communication volume of the OTIS is obtained as:

$$V_{OTIS} = \frac{4\lambda^3}{\pi^2}\left(\frac{2m+4}{m}\right)\eta_1\eta_3 NM\sqrt{N}\sqrt{M} f_{\#1} f_{\#3} \tag{16}$$

The physical volume of the OTIS is equal to:

$$L = \frac{8\lambda}{\pi}\left(\frac{2m+4}{m}\right)\eta_1\eta_3\sqrt{N}\sqrt{M} f_{\#1} f_{\#3} \tag{17}$$

Therefore, the physical volume of the OTIS is given as:

$$V = \left(\frac{256\lambda^2}{\pi^3}\right)\left(\frac{2m+4}{m}\right)\eta_1\eta_3 (NM)^{3/2} f_{\#1}^2 f_{\#3}^2 \tag{18}$$

The ratio between the physical volume and the optical communication volume is approximately:

$$\frac{V}{V_{OTIS}} \approx f_{\#1} f_{\#3} \tag{19}$$

For $f_{\#1} = f_{\#3} = 1$, the physical volume is approximately equal to the optical communication volume, implying that a cross-sectional area of each optical interconnection in the system is of $\approx \lambda^2$. That is the OTIS system is capable of nearly achieving the fundamental minimum volume.

7. Conclusions

In this paper the optical transpose interconnection system has been explored. The operation of the transposition of the overall optical system is performed using the three stages of lenses without requiring beam steering components at the input plane and at the output plane. Thus the system suffers from the intrinsic aberrations due to the lenses of the system. Most aberrations of the system come expectedly from a macrolens in stage II. To overcome these problems a compound lens system, which replaces the single macrolens stage II, is used. The aberrations of the system is derived by using Lie Methods and classified as different types of aberrations such as spherical aberration, coma, astigmatism, and distortion.

By using the scaling law it is shown that the physical volume of the optical transpose interconnection system is equal to the optical communication volume, that is the optical transpose interconnection system can be scaled down to the size of wavelength.

Each of the switches discussed in this paper utilizes such an optical transpose interconnection system invented in this project to provide optical switches having improved properties. Each of the optical crossbar switches described in this paper could be configured as a fixed arbitrary interconnection, or as a reconfigurable interconnection. In the former case, the deflectors would be configured by using a deflection technology. Computer generated holography [8,9] is a suitable technology for such deflectors. It is also possible to use other deflection technology such as micromirrors (MEMS technology [10,11]), prisms and beam splitters. Liquid crystal devices that act as variable gratings, prisms and even lenses can be used in the reconfigurable interconnections. SLMs [12] can also be used as programmable CGH deflectors, that is as variable grating. SLMs can be transmissive or reflective.

Overall, this system produces the Fourier transform, at the output, of a beam at the associated input. Conventional systems would, on the other hand, image. However, by suitable choice of lenses, it is possible to arrange that the size and numerical apertures of the beams at the input and the output are identical, allowing interfacing with optical fibres without loss in principle. In particular, in the case of monomode

beams, a Gaussian input beam is transformed to a Gaussian output beam.

8. References

[1] David A. B. Miller, *Physical reasons for optical interconnection*, International J. of Optoelectronics, Vol.11, pp.155-168, 1997.

[2] Michael R. Feldman, Clark C. Guest, Timothy J. Drabik, and Sadik C. Essener, *Comparison between electrical and free space optical interconnects for fine grain processor arrays based on interconnect density capabilities*, Applied Optics, Vol.28, pp.3820-3829, 1989.

[3] G. C. Marchand, P. Harvey, and S. C. Essener, *The Optical Transpose Interconnection System Architectures*, Optics Letters, Vol.18, pp.1083-1085, 1993.

[4] Predrag Milojkovic, Marc P. Christensen, and Michael W. Haney, *Minimum Lens Complexity Design Approach for a Free-space Macro-optical Multi-chip Global Interconnection Module*, Optics in Computing 2000, SPIE, Vol.4089, pp.917-926, 2000.

[5] Tetsundo Sekiguchi and Kurt Bernardo Wolf, *The Hamiltonian formulation of optics*, Am. J. Phys., Vol.55(9), pp.830-835, 1987.

[6] LightTools is an illumination design program based on 3D interactive solid modelling with optical accuracy. The software is developed by Optical Research Associates, www.opticalres.com.

[7] BK7_SCHOTT has the glass type designation 517642, i.e., refractive index 1.517, Abbe number 64.2.

[8] Ren ChaoHong, Zhou Jin, and Gao WenQi, *Four-channel self-focus computer-generated hologram*, Applied Optics, Vol. 36, pp.8844-8847, 1997.

[9] Jean-Numa Gillet and Yunlong Sheng, *Multiplexed Computer-Generated Hologram with Polygonal Apertures*, Applied Optics, Vol.41, pp.298-307, 2002.

[10] U. Krishnamoorthy, M. Han, D. Lee, Y-A. Peter, H. Wada, K. Yu, and O. Solgaard, *Optical Internet: the next generation All-Optical MEMS Fiber Switches*, Stanford University, California, U.S.A., May 23, 2001.

[11] Paul M. Hagelin, Uma Krishnamoorthy, Johnathan P. Heritage, and Olav Solgaard, *Scalable Optical Cross-Connect Switch Using Micromachined Mirrors*, IEEE Photonics Technology Letters, Vol.12, No. 7, pp.882-884, 2000.

[12] Fai Mok, Joshep Diep, Kua-Kuang Liu, and Demetri Psaltis, *Real-time computer-generated hologram by means of liquid-crystal television spatial light modulator*, Optics Letters, Vol.11, pp.748, 1986.

[13] Haldun M. Ozaktas, Hakan Urey, and Adolf W. Lohmann, *Scaling of diffractive lenses for optical computing and interconnections*, Appl. Opt., Vol.33, pp.3782-3789, 1994.

Wanchai Pijitrojana received the B.Eng. degree in Telecommunication Engineering from King's Mongkut Institute of Technology, Ladkrabang, Bangkok, Thailand. He also received the M.S. degree in both, Computer Technology and Nonlinear Optics (Electrophysics) from Asian Institute of Technology, Bangkok, Thailand and the University of Southern California, California, U.S.A., respectively, and the Ph.D. degree in Optoelectronics from King's College, University of London, London, England. He is currently a lecturer in the EE Department, Thammasat University, Bangkok, Thailand. His current research interests are Optical Interconnection systems, Optical Design, Optics, Nonlinear Optics, Physical Optics, PBG, and Mathematics applied to Optics.

Trevor J. Hall received the Ph.D. degree in fibre optics from University of College London in 1980.

In 1984, he joined King's College London. In 1994, he was promoted to Professor of Optoelectronics at King's College London. He has been a professor at the University of Ottawa since 2002. His research interests include Optical Communication Systems, Optoelectronic Packet Switches, Photonic Technology & Optical Physics, Models of Internet Topology, and Dynamic of the Internet. He has over 200 publications including 100 papers in journals. He is author of five patents on packet switch architecture and allied optoelectronic technology.